JOURNAL OF MATERIALS SCIENCE **34** (1999) 1799–1807

Creep behavior in SiC-whisker reinforced silicon nitride composite

S. ZHU*‡, M. MIZUNO*, Y. KAGAWA‡
*Japan Fine Ceramics Center, Atsuta-ku, Nagoya, 456-8587, Japan
‡Institute of Industrial Sciences, The University of Tokyo, Tokyo, 106, Japan
E-mail: zhu@mce.uec.ac.jp

H. KAYA
Petroleum Energy Center, Minato-ku, Tokyo, 105-0001, Japan

Tensile and flexural creep tests of 20 vol % SiC whiskers reinforced Si_3N_4 composite processed by gas pressure sintering have been carried out in air in the temperature range of 1000–1300 °C. The stress exponent for flexural creep is 16 at 1000 °C. However, at 1200 and 1250 °C the stress exponents for both tensile and flexural creep vary with increasing stress. In the low stress region, the activation energy for creep is 1000 kJ/mol. In the high stress region, it is 680 kJ/mol. The different creep mechanisms dominate in the low and high stress regions, respectively.

1. Introduction

Creep behavior of monolithic silicon nitride have been widely studied since 1970s [1–4]. The Si_3N_4 grains are separated by amorphous phases, which are the remnants of the sintering aid and SiO_2 coated the original Si_3N_4 particles [5]. Creep deformation occurs at high temperature when the amorphous grain boundary phase softens, thus permitting relative motion of the grains. Improvement of the refractoriness of the sintering aid and reduction of the amount of the sintering aid have dramatically improved the creep resistance of silicon nitride.

In recent years, silicon nitride matrix composites were developed for increasing fracture toughness, thermal shock resistance and creep resistance [6–8]. SiC whiskers reinforced silicon nitride is one of such advanced composites. The addition of SiC whiskers can markedly increase fracture toughness and thermal shock resistance [9–12]. However, the effects of SiC whiskers on creep resistance are contradictory [13–16]. A considerable improvement in flexural creep resistance was observed at 1200 °C when 30 vol % SiC whiskers were added to silicon nitride [13]. Ohji *et al*. [14] also observed the better creep resistance in 20 wt % SiC whiskers reinforced Si_3N_4 in tensile creep at 1200 °C, but the superiority disappeared above 1300 °C. However, in both the 20 and 30 vol % SiC whiskers reinforced silicon nitride, compressive creep rates were higher than those in the unreinforced materials in the temperature ranges of 1200–1300 °C, but creep resistance of the composites was the same as, or higher than the unreinforced materials at 1300–1400 °C [15]. Under all the conditions, creep rate of the 30 vol % material is lower than that of the 20 vol % material [15]. Little effect was also found on tensile creep resistance at 1250 °C [16].

One of the reasons for the unimprovement is that the unreinforced material contained an appreciable concentration of elongated grains of β-Si_3N_4, which increased both the fracture resistance and the creep resistance of the material [16]. The addition of SiC whiskers to the silicon nitride powders effectively replaces the elongated β-Si_3N_4 grains with the SiC whiskers. If the whiskers and elongated β-Si_3N_4 grains act in a similar manner during creep, then little change in creep resistance is expected by replacing elongated silicon nitride grains with SiC whiskers. Another reason is caused by the additional SiO_2 contributed by the SiC whiskers to the overall grain boundary glass composition and the resultant decrease in the vol % of crystallization in this area [15]. Moreover, the Ca is introduced in the composite by adding whiskers, decreasing the effective viscosity of the intergranular phase, thereby decreasing the resistance of the composite to creep [16]. Based on these arguments, it is expected that the creep resistance of the composite will be higher if the whiskers are kept with higher aspect ratio than elongated β-Si_3N_4 grains and the compositions are strictly controlled during processing to avoid the harmful impurities. Moreover, there is little research on the effects of SiC whiskers on creep cavitation and the creep fracture mechanisms [16, 17]. Most SiC whisker reinforced silicon nitride composites are processed by hot-pressing [9, 10, 13–16] to increase density, but the hot-processing is limited to simple shapes and its fabrication cost is high. Cost-effective processing is necessary to expand the application of silicon nitride composites. Slip casting and pressureless sintering are recently used to fabricate SiC_w/Si_3N_4 composite [12, 17, 18], and good mechanical properties and excellent thermal shock resistance are achieved [12]. We selected this kind of SiC_w/Si_3N_4 to study creep behavior in both flexure and tension at the temperatures

from 1000 to 1300 °C. The effects of SiC whiskers on creep resistance are examined by microscopic observation and analysis. Creep mechanism of SiC_w/Si_3N_4 is also explored.

2. Materials and experimental procedures

Gas pressure sintered silicon nitride (Japan Metals & Chemicals Co., Tokyo, Japan) reinforced with 20 vol % SiC whiskers (Tokai Carbon Co., Tokyo, Japan) was used for the investigation. The average diameter and length of the whiskers were 1.3 and 10–50 μm, respectively. The additives were a mixture of yttria, alumna and cordierite, totally 12% in weight. The sintering conditions were at 1825 °C and in 1 MPa nitrogen for 2–4 h [12].

Flexural creep tests were carried out using an Instron testing system (Model 1381, Instron Co., MA, USA) in air at 1000 and 1200 °C. The fluctuation of the testing temperature was within ±1 °C. The four point flexural specimens had the dimensions of 3 × 4 × 40 mm. The inner roller span was 10 mm and the outer 30 mm. Creep strain was measured by linear variable differential transducer.

Tensile creep tests were carried out using a constant load creep machine (Mode HTT-300, Toshin Kogyo Co. Ltd., Tokyo, Japan) in air at the temperatures of 1150, 1200, 1250 and 1300 °C. The stress increase test in a single specimen was conducted, i.e., the stress increased when steady state creep stage reached. The tensile specimens had a gage length of 25 mm with a cross section of 2.5 × 4.0 mm (Fig. 1). The alignment of the tensile specimens was adjusted to a bending strain less than 5% using 4 strain gages attached to side faces of the gage portion in specimen at room temperature before creep tests. Creep strain was measured by Zimmer Digital Extensometer (Model 4100, Karl. F. Zimmer KG, Rossdorf/Darmstadt, Germany).

Microstructures of specimens were observed by optical microscope and scanning electron microscope (SEM). The plasma etching technique was used to reveal grain boundaries of Si_3N_4 and to distinguish SiC whiskers from the elongated Si_3N_4 grains. Cavities in crept specimens were examined using SEM on both side surfaces and on new fracture surfaces generated at room temperature in the gage section. Some fracture surfaces at elevated temperatures were etched in molten potassium and sodium hydroxides (1 : 1) at 300 °C for 30 s to remove glassy phases.

3. Results and discussion

3.1. Microstructure

The microstructures of the matrix consisted of elongated Si_3N_4 grains with an aspect ratio of about 4

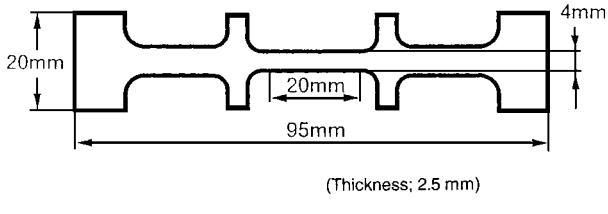

Figure 1 Shape and dimensions of tensile creep specimen.

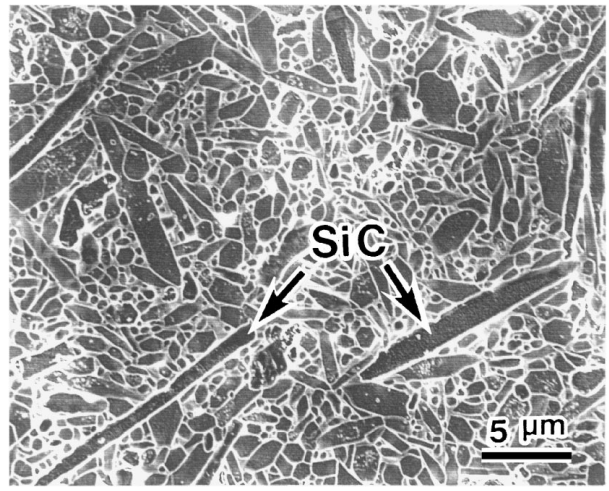

Figure 2 Microstructure of SiC_w/Si_3N_4 composite in original state.

(Fig. 2) and equiaxed Si_3N_4 grains in a diameter of 0.2–1 μm [19]. The average diameter and length of SiC whisker were 1.3 and 9 μm, respectively.

3.2. Flexural creep

Creep strain versus time curves at 1000 and 1200 °C are shown in Fig. 3. It can be seen that creep strain increases with increasing stress at both the temperatures. There are primary (transient) and secondary creep stages, but no tertiary creep stage appears at any testing conditions. Creep rupture occurs at the early transient creep stage at the high stresses. At 1200 °C, when the stresses are higher than 170 MPa, creep strain almost linearly increases with time and then the specimen failed (Fig. 3b). Since the steady state creep does not occur at the high stresses, the minimum creep strain rates are used to analyze creep deformation behavior.

Fig. 4 shows the minimum creep strain rates as a function of stress at the two temperatures. Creep strain rate can be described by the power law equation

$$\dot{\varepsilon} = A \cdot \sigma^n \cdot \exp(-Q/RT) \qquad (1)$$

where A is a constant, n is the apparent stress exponent for creep, Q is the apparent activation energy for creep, R is gas constant and T is the absolute temperature. The stress exponent for creep is 16 at 1000 °C. However, at 1200 °C the stress exponents for creep are 2 in the low stress (below 170 MPa) region and 4 in the high stress (above 170 MPa) region at 1200 °C. There is a gap in creep rate between the low stresses and high stresses at 1200 °C, which covers two orders of magnitude in creep rate. This is an unusual phenomenon for creep of silicon nitride. To understand this mechanical behavior, tensile creep rests were conducted at 1150–1300 °C. The results will be stated in the following section.

The different stress exponents for creep between 1000 and 1200 °C mean that the creep mechanisms may be different. Also, the creep rate versus time to rupture curves at the two temperatures are separate each other (Fig. 5). This further demonstrates the different creep mechanisms between 1000 and 1200 °C. The observation on the creep damage and the crack

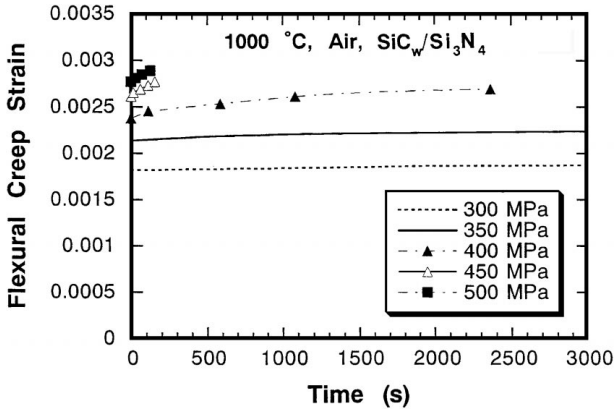

(a)

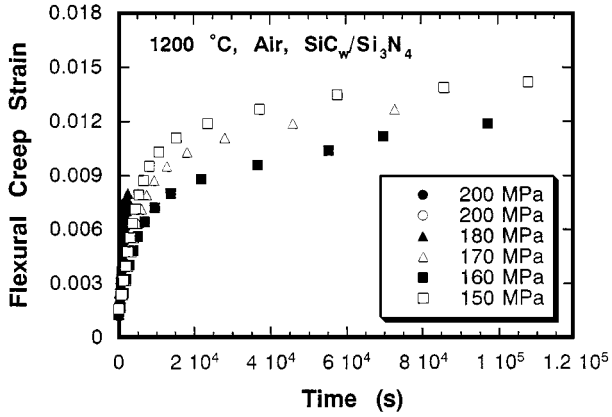

(b)

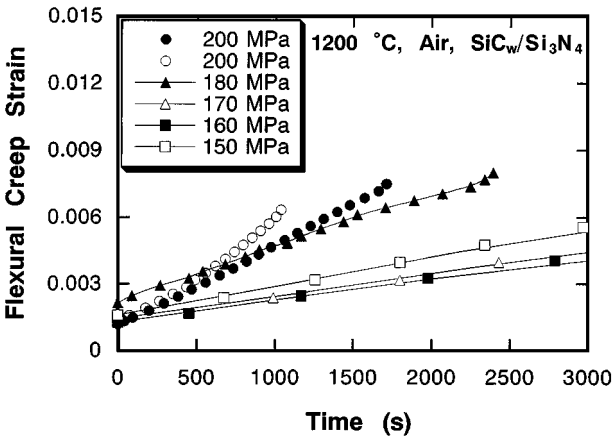

(c)

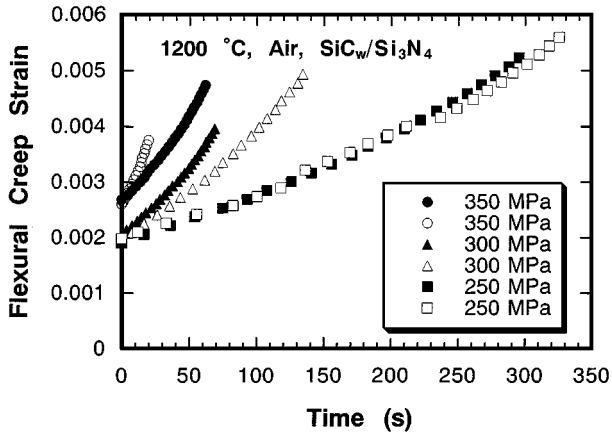

(d)

Figure 3 Flexural creep strain versus time at 1000 and 1200 °C.

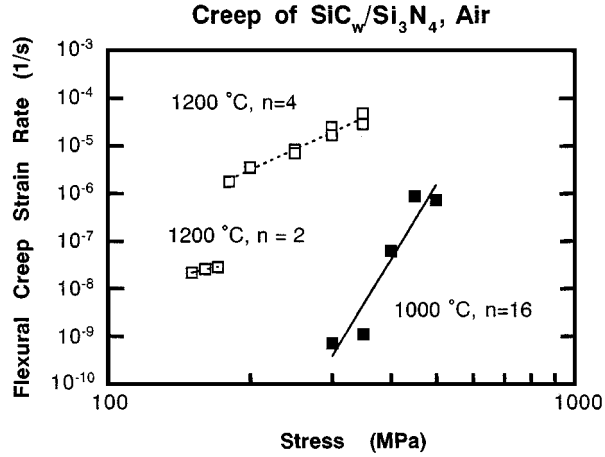

Figure 4 The minimum creep strain rate as a function of stress in flexural creep at 1000 and 1200 °C.

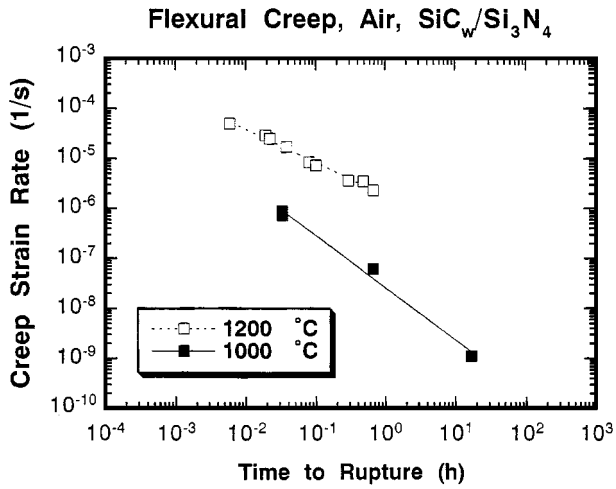

Figure 5 The minimum creep strain rate versus time to rupture in flexural creep at 1000 and 1200 °C.

propagation paths also proves this argument as described in the Section 3.4.

3.3. Tensile creep

The curves of the tensile creep strain versus time at 1200, 1250 and 1300 °C are shown in Fig. 6. At 1200 °C, no tertiary creep stage exists at any stress, similar to the flexural creep. However, there are tertiary creep stages at low stresses at 1250 and 1300 °C.

The minimum creep strain rate as a function of stress is shown in Fig. 7. At 1200 and 1250 °C, the stress exponent for tensile creep is 4 in the high stress region, which is the same as the stress exponent for flexural creep. The specimens fracture in the early transient stage in the high stress region (Fig. 6). If the specimen fractures in the secondary stage its creep rate is much lower (see the two data at 60 MPa at 1250 °C). The stress exponent for tensile creep in the low stress region is 6, which is higher than that for flexural creep. At 1150 and 1300 °C, there is no high stress region. The gap in creep rate between the low and high stresses at 1200 and 1250 °C also covers two orders of magnitude in creep rate as in Fig. 4. If the stress exponent in the gap is calculated, it is 20, unrealistic high value.

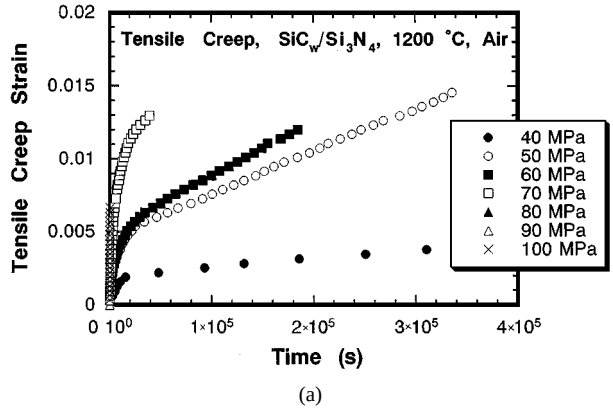

(a)

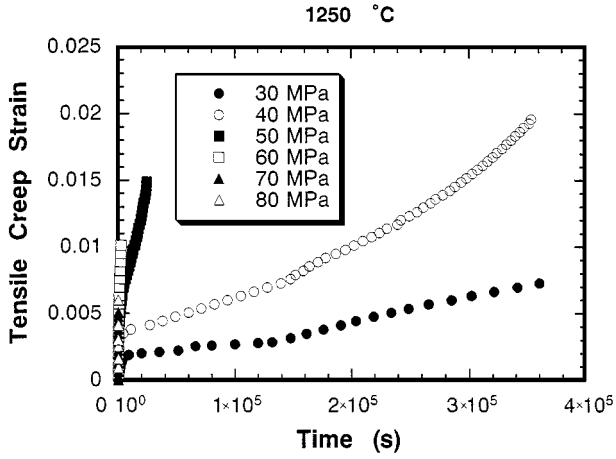

(b)

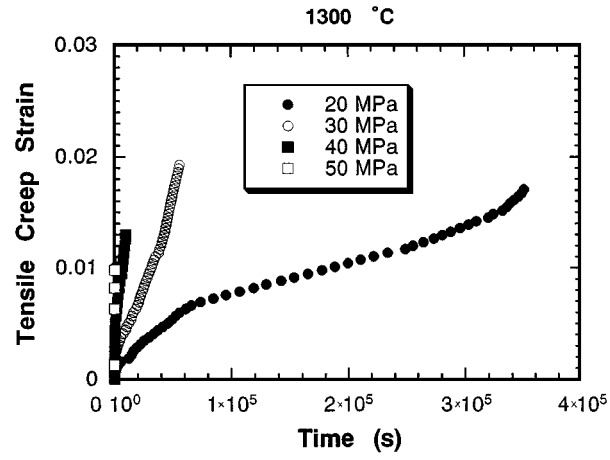

(c)

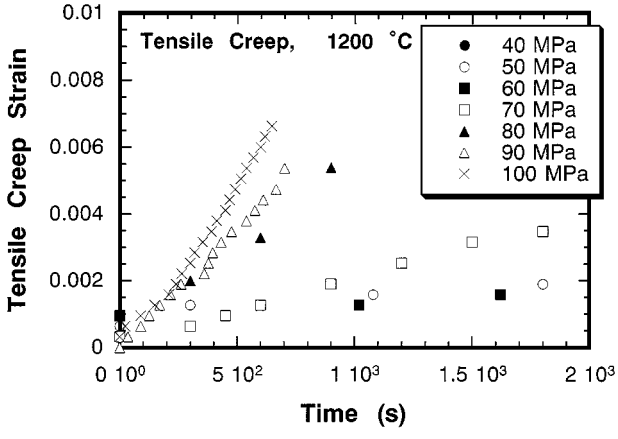

(d)

Figure 6 Tensile creep strain versus time at 1200, 1250 and 1300 °C.

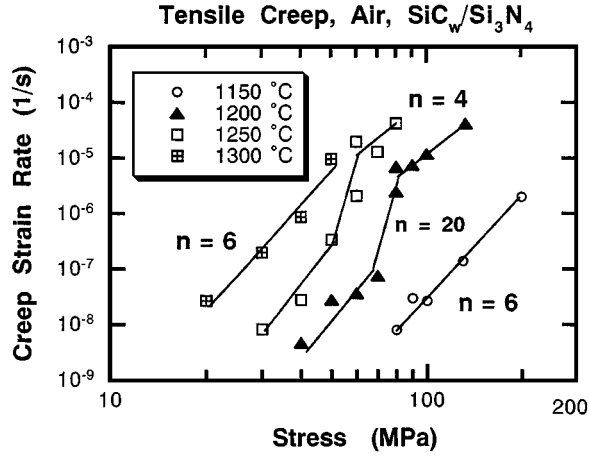

Figure 7 The minimum creep strain rate as a function of stress in tensile creep at 1150, 1200, 1250 and 1300 °C.

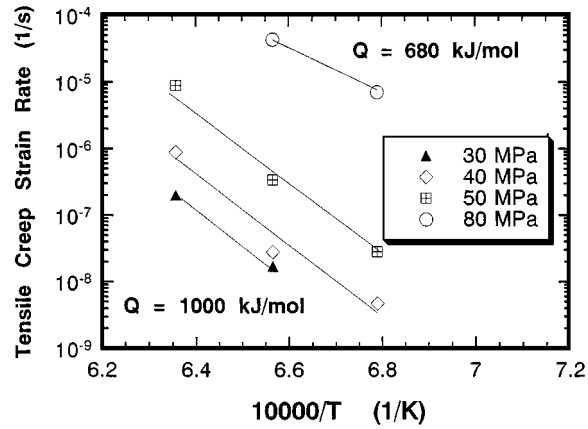

Figure 8 The minimum creep strain rate as a function of absolute temperature in tensile creep.

The minimum creep strain rate as a function of the absolute temperature is shown in Fig. 8. The activation energy for creep can be obtained by the data at the same stress. In the low stress (50 MPa) region, the activation energy for creep is about 1000 kJ/mol. In the high stress (80 MPa) region, it is about 680 kJ/mol. At 60 MPa or 70 MPa, it is even 1900 kJ/mol, since the data belong to the different creep regions. This demonstrates that the different creep mechanisms may dominate in the low and high stress regions, respectively.

3.4. Creep cracks and fracture surfaces

Crack propagation at 1000 °C is both intergranular and intragranular in mode (Fig. 9). SiC whiskers are often broken and microcracks in front of the main crack are wedgeshaped. However, crack propagation at or above 1200 °C is intergranular and is a process of cavity nucleation, growth and interlinkage, as shown in Fig. 10. Longitudinal SiC whiskers or elongated Si_3N_4 grains can prohibit the interlinkage of cavities or opening of cracks. Whisker-bridging may be an important operative mechanism for increasing fracture resistance at the temperatures above 1200 °C. Cavities are roundshaped and nucleated in glassy phases on grain boundaries. The crack opening displacement and the roughness of crack face above 1200 °C are greater than those at 1000 °C.

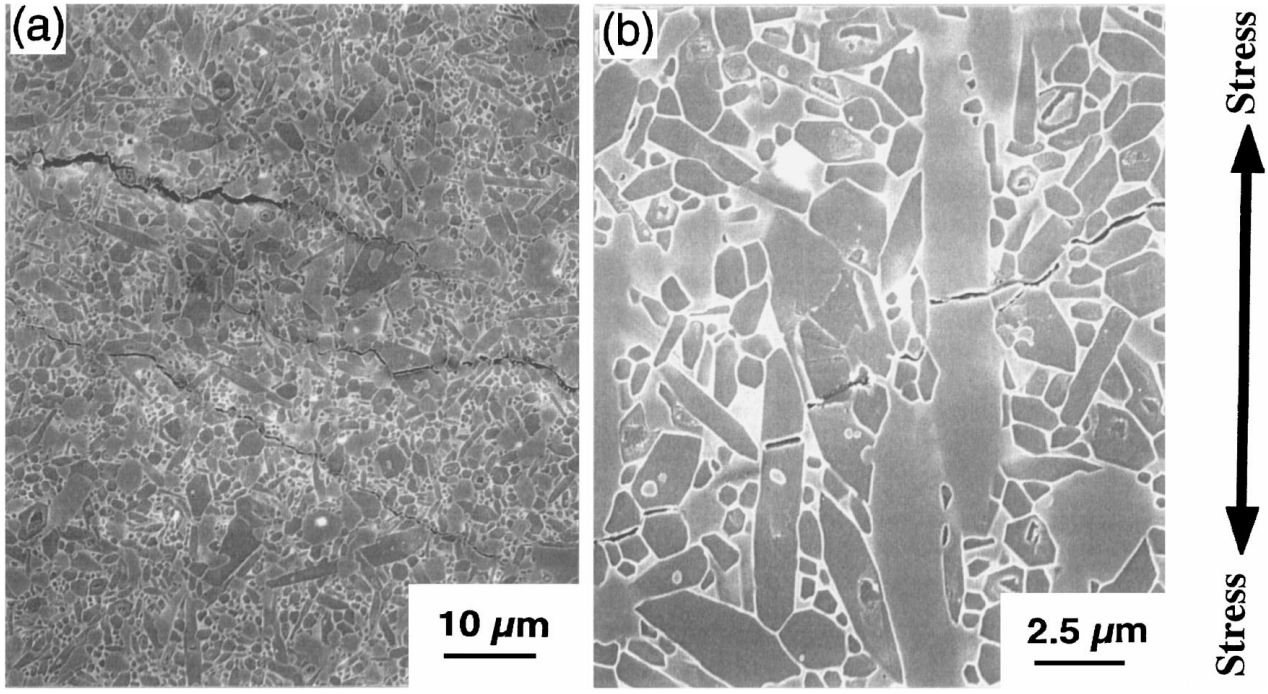

Figure 9 Crack propagation in flexural stress rupture at 1000 °C and 400 MPa for 40 min.

On fracture surfaces generated at room temperature after creep tests, no cavity on grain facets was observed for creep specimens at either 1200 or 1300 °C. This demonstrates that the cavities shown in Fig. 10 are indeed within glassy phases.

The flexural rupture surfaces at 1000 °C consist of mirror, mist and hackle regions (Fig. 11a). The size of the mirror region increases with decreasing stress. Unlike the rupture at 1000 °C, a rough zone (creep damage area) is visible and the mirror zone covers the rest area of the rupture surface for both the flexural and tensile creep at the temperature 1200 °C (Fig. 11b,c). At 1150 °C and 200 MPa, the tensile creep rupture surface consists of rough zone, and mirror and hackle zones (Fig. 12a). However, at 1200 °C, even in monotonic tension, there is no hackle pattern on the fracture surfaces (The ultimate tensile strength is 132 ± 3 MPa.) (Fig. 12b). Creep crack growth occurs in the rough zone [17]. When the crack length reaches the critical crack length, the fast crack growth leads to fracture. Wereszczak *et al.* [3] calculated the stress intensity by measuring the size of the rough zone, which was close to the high temperature fracture toughness. This method was applied to the present experimental results. The size of the rough zone on the tensile creep rupture surfaces and the calculated critical stress intensity are shown in Table I. It can be seen that the calculated stress intensities are not constant and unrealistically large for the big size of the rough zone. Even if the data for $a/W > 0.6$ are not considered due to inaccuracy [20], the critical stress intensities are still too large.

3.5. Creep deformation mechanism

Several creep deformation mechanisms in silicon nitride have been proposed in the past two decades. Three of them are mostly accepted, i.e., viscous flow of glassy phases from compressive boundaries to tensile boundaries [21, 22]; solution-reprecipitation by

TABLE I Size of rough zone on tensile creep rupture surfaces and critical stress intensity (K_c)

Temperature (°C)	Stress (MPa)	Width (W) (mm)	Thickness (mm)	Size (a) (mm)	a/W	K_c (MPa m$^{1/2}$)
1200	100	3.948	2.316	1.318	0.33	11.40
1200	90	3.947	2.315	1.733	0.44	15.60
1200	80	3.915	2.326	1.702	0.43	13.35
1200	70	3.95	2.316	2.004	0.51	16.22
1200	60	3.928	2.312	2.195	0.56	17.30
1200	50	3.939	2.303	2.387	0.61	18.10
1250	80	4.037	2.451	1.376	0.34	9.54
1250	70	4.043	2.478	1.899	0.47	13.89
1250	60	4.046	2.469	2.092	0.52	14.69
1250	60	4.035	2.453	2.228	0.55	16.82
1250	50	3.994	2.485	3.631	0.91	75.38
1300	50	3.945	2.326	3.179	0.8	45.03
1300	40	4.032	2.453	4.032	1	90.51
1300	30	3.948	2.316	3.948	1	67.17

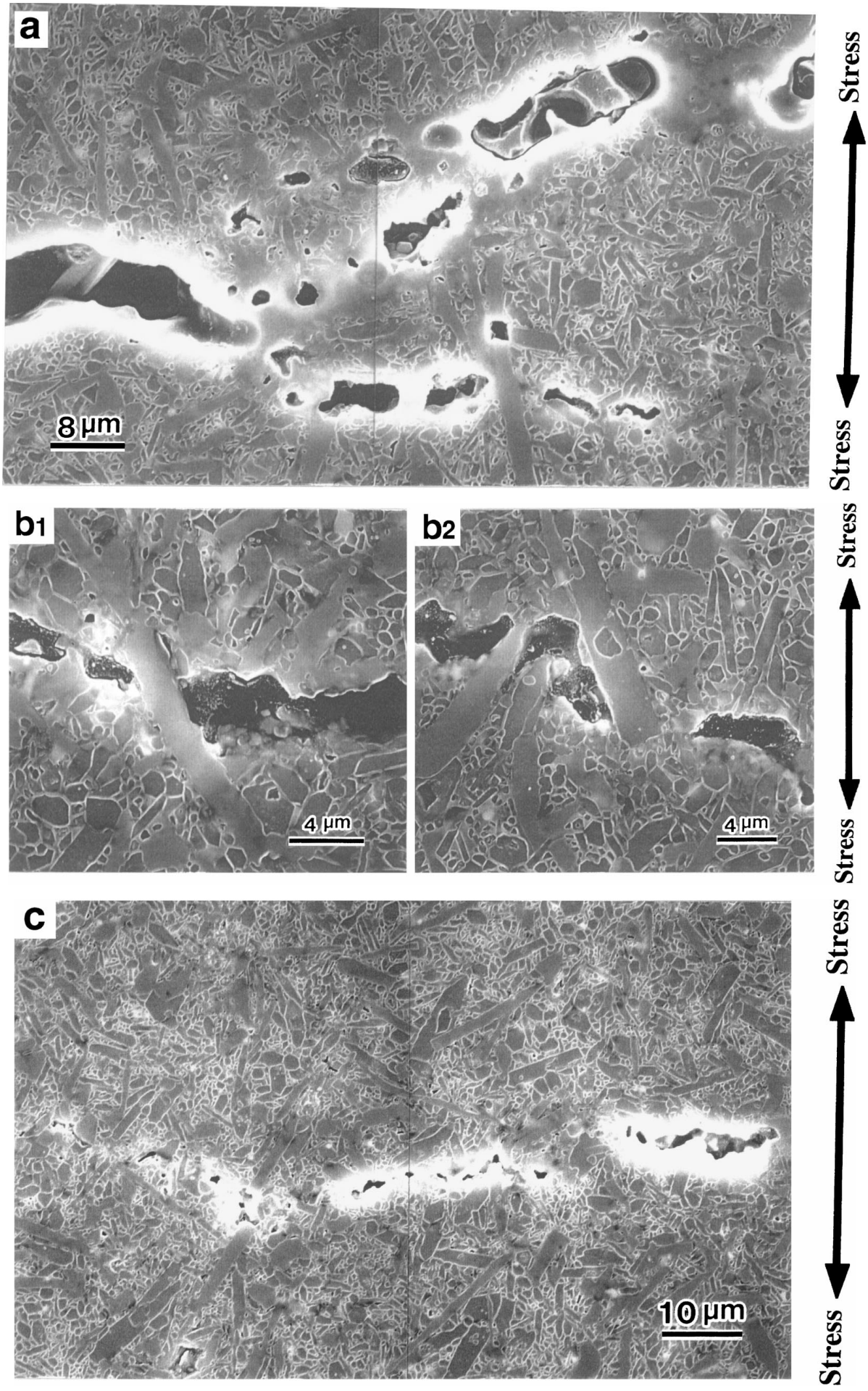

Figure 10 Crack propagation in tensile creep. (a) 1200 °C and 50 MPa for 93.7 h; (b1) and (b2) 1250 °C and 50 MPa for 7 h; (c) 1300 °C and 30 MPa for 16.2 h.

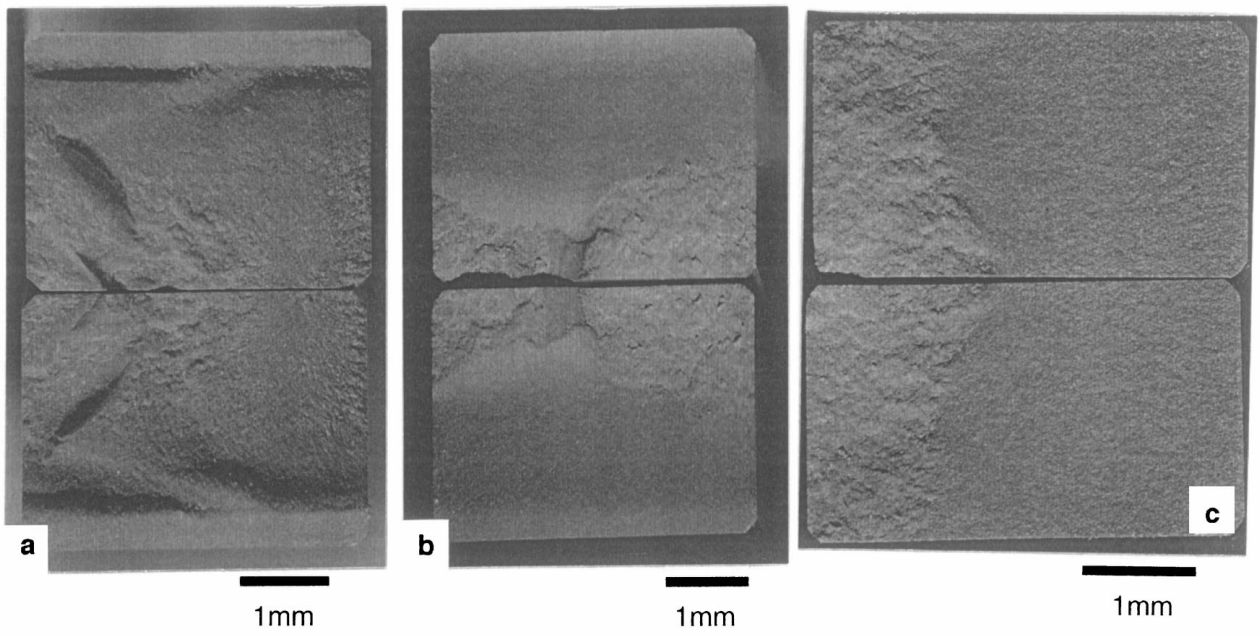

Figure 11 Fracture surfaces: (a) flexural creep at 1000 °C and 500 MPa for 0.03 h; (b) flexural creep at 1200 °C and 200 MPa for 0.35 h; (c) tensile creep at 1200 °C and 100 MPa for 0.17 h.

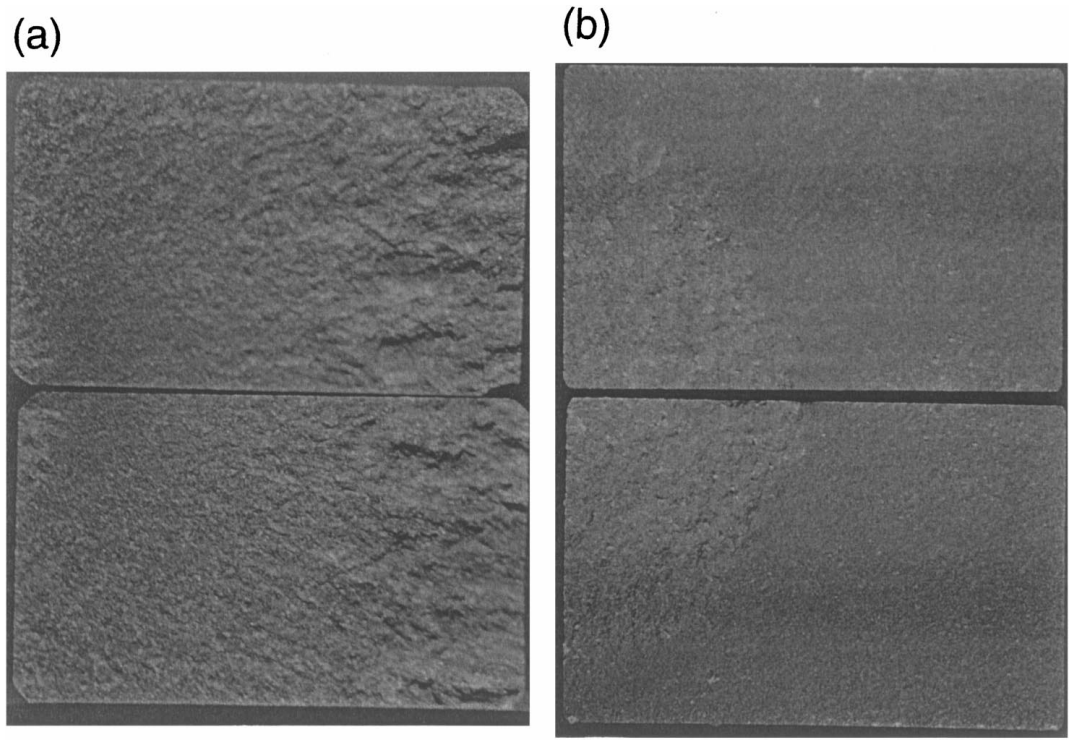

Figure 12 (a) Stress rupture surface in tensile creep at 1150 °C and 200 MPa for 0.06 h; (b) Tensile fracture surface at 1200 °C with loading rate of 0.05 mm/min.

dissolving Si_3N_4 grains into the glassy phases at some boundaries and reprecipitating the glassy phases onto the Si_3N_4 grains at others [23]; and cavitation [4, 24, 25].

Among these mechanisms, grain boundary sliding and viscous flow are likely to be responsible for the high creep rate during primary creep. It can be found that all the specimens at high stresses were broken at the near-linear part (constant creep rate) of the creep strain-time curves at 1200 and 1250 °C (Figs 3 and 6). It was reported that the constant initial creep rate exhibited a stress exponent of 4 and an activation energy of 700 kJ/mol and the initial creep behavior is controlled by viscous flow in a silicon nitride (SN220) [22]. When this process is exhausted by grain impingement, creep rate decreases. The maximum strain limit for the

viscous flow in tension predicted by Dryden *et al*. [21] is $\varepsilon_{max} = \delta/d$, where δ is the grain boundary phase thickness and d is the grain size. In the current material with $d = 0.2$–1 μm and $\delta = 1$ nm [19]. This limit requires the maximum strain of 0.001–0.005, which is consistent with the value at high stresses. The specimens at high stresses fracture before the decrease in creep rate at 1200 and 1250 °C. However, at higher temperatures (i.e., 1300 °C) the viscosity of the grain boundary film is low, and thus this process is exhausted so quickly that it becomes part of the loading transients. In this case the materials appear not to exhibit exhaustion creep processes [22].

The tensile creep in the low stress region has the stress exponent ($n = 6$) and activation energy (1000 kJ/mol) similar to the values for the tensile creep of monolithic Si_3N_4 [2] and SiC_w/Si_3N_4 composites [15, 16]. The stress-enhanced solution reprecipitation mechanism predicts the creep rate to be linearly related to the applied stress and can not be used in an unaltered form to explain the nonlinear aspects of creep as observed in this study and other studies. Hockey *et al*. [16] found that the creep stress exponent under tensile loading was 5.9, whereas under compressive loading it was 1. Microscopic study showed extensive cavitation at the whisker-silicon nitride interfaces under tension and absence of cavitation under compression. The microstructural observations revealed the presence of cavities in the grain boundary second phase (Fig. 10). Therefore, the high stress exponent and activation energy for the tensile creep may be an apparent phenomenon by cavitation compared to the compression creep [4, 16]. Once cavities are formed, the creep rate then increases as a result of both cavity nucleation and growth. Since the rate of the nucleation and growth of cavities is a nonlinear function of applied stress, the creep process also becomes a nonlinear function of stress [16]. However, the stress dependence of the creep rate is not directly calculable, since it depends essentially on the distribution of grain pockets favorably oriented for cavitation [4].

3.6. Life prediction

Fig. 13 shows the relationship of the minimum creep strain rate with the time to rupture. All the data at

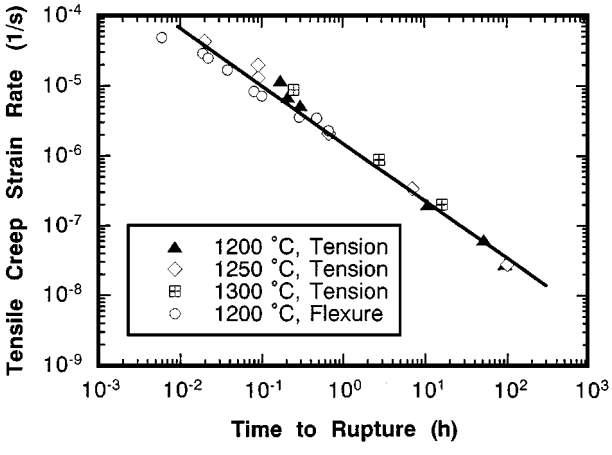

Figure 13 The minimum creep strain rate versus time to rupture in tensile creep at 1200, 1250 and 1300 °C and flexural creep at 1200 °C.

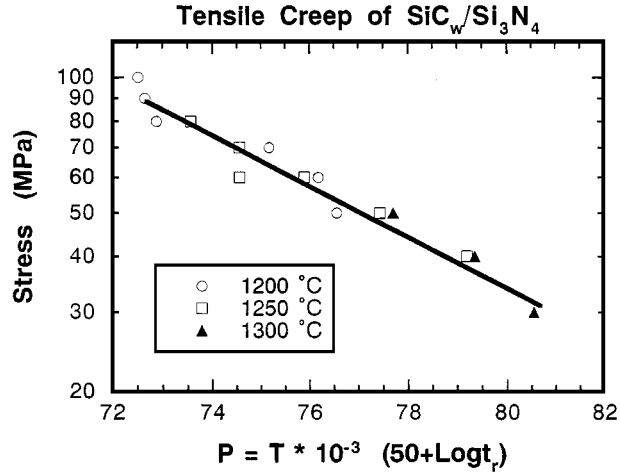

Figure 14 Larson-Miller curve for tensile creep at 1200, 1250 and 1300 °C.

the three temperatures fall on the same line, i.e., fit Monkman-Grant relation [26]

$$t_r \cdot \dot{\varepsilon}^m = C_{M\text{-}G} \tag{2}$$

where m is the strain rate exponent and $C_{M\text{-}G}$ is a constant. It is noted that the data of the flexural creep at 1200 °C also fall on the same line as the tensile ones. If the value of m is equal to 1, the failure stain is relatively constant, irrespective of applied stress or temperature. Fig. 13 shows that m is 1.25, which is between the values of 1 by Ohji and Yamauchi [15] and 1.69 by Hockey *et al*. [16].

Monkman-Grant relationship is a useful way for life design and residual life prediction for engineering components (Fig. 13). This method is based on the measurement of creep strain rate. For engineering components, sometime it is impossible to measure creep strain rate. In this case, it is better to use the Larson-Miller parameter for residual life prediction.

Larson-Miller parameter (P) [27] is one of the useful parameters used for predicting creep life in metallic materials. The basic assumptions of it are that $m = 1$ and Q is a function of stress. The present results are approximately satisfied with these assumptions. It can be used for correlating stress-temperature-life relationship in SiC_w/Si_3N_4 composite in the following expression:

$$P = T(C + \log t_r) \tag{3}$$

The constant (C) of Larson-Miller parameter is 20 for metals and alloys. For monolithic silicon nitride, it is among 30 and 40, depending on grades of silicon nitride [28, 29]. The values of the constant for SiC_w/Si_3N_4 composite are 50, determined by fitting the data at three temperatures (Fig. 14).

4. Conclusion

The stress exponent for flexural creep is 16 at 1000 °C. However, at 1200 and 1250 °C the stress exponents for both tensile and flexural creep vary with increasing stress. In the low stress region, the specimens fracture

at the secondary or tertiary stage and the activation energy for tensile creep is 1000 kJ/mol. In the high stress region, the specimens fracture at the primary stage and the activation energy for tensile creep is 680 kJ/mol. The exhaustion creep mechanism dominates in the high stress regions. At 1300 °C, the viscosity of the grain boundary film is low, and thus the exhaustion process is so quick that it becomes part of the loading transients. Creep strain rate in the low stress region is controlled by the solution-reprecipitation mechanism.

Acknowledgements

We are very grateful for the assistance of Mr. K. Shirai, Mr. Y. Nagano and Dr. F. Lofaj in the mechanical tests. Thanks to Mr. A. Suda in Toyota Central R & D Labs. and to Dr. T. Nishimura in NIRIM for the plasma etching. This work is a part of the automotive ceramic gas turbine development programs conducted by Petroleum Energy Center, Japan.

References

1. W. R. CANNON and T. G. LANGDON, *J. Mater. Sci*. **18** (1983) 1.
2. M. K. FERBER and M. G. JENKINS, *J. Amer. Ceram. Soc*. **75** (1992) 2453.
3. A. A. WERESZCZAK, M. K. FERBER, T. P. KIRKLAND, K. L. MORE, M. R. FOLEY and R. L. YECKLEY, *ibid*. **78** (1995) 2129.
4. W. E. LUECKE, S. M. WIEDERHORN, B. J. HOCKEY, R. F. KRAUSE, JR. and G. G. LONG, *ibid*. **78** (1995) 2085.
5. D. R. CLARKE and G. THOMAS, *ibid*. **60** (1977) 491.
6. YU. G. GOGOTSI and G. GRATHWOHL, *J. Mater. Sci*. **28** (1993) 4279.
7. J. W. HOLMES, *ibid*. **26** (1991) 1808.
8. R. B. THAYER and J.-M. YANG, *Mater. Sci. Eng*. **A160** (1993) 169.
9. P. D. SHALEK, J. J. PETROVIC, G. F. HURLEY and F. D. GAC, *Amer. Ceram. Soc. Bull*. **65** (1986) 351.
10. S. G. BULJAN, J. G. BALDONI and M. L. HUCKABEE, *ibid*. **66** (1987) 347.
11. T. KANDORI, S. KOBAYASHI, S. WADA and O. KAMIGAITO, *J. Mater. Sci. Lett*. **6** (1987) 1356.
12. T. YONEZAWA, S. SAITOH, M. MINAMIZAWA and T. MATSUDA, *Compos. Sci. Technol*. **51** (1994) 265.
13. J. G. BALDONI and S.-T. BULJAN, "Ceramic Materials & Components for Engines," edited by V. J. Tennery (American Ceramic Society, Columbus, Ohio, 1989) p. 786.
14. R. D. NIXON, D. A. KOESTER, S. CHEVACHAROENKUL and R. F. DAVIS, *Compos. Sci. Technol*. **37** (1990) 313.
15. T. OHJI and Y. YAMAUCHI, *J. Amer. Ceram. Soc*. **76** (1993) 3105.
16. B. J. HOCKEY, S. M. WIEDERHORN, W. LIU, J. G. BALDONI and S.-T. BULJAN, *J. Mater. Sci*. **26** (1991) 3931.
17. S. ZHU, M. MIZUNO, Y. NAGANO, Y. KAGAWA and M. WATANABE, *J. Amer. Ceram. Soc*. **79** (1996) 2789.
18. M. J. HOFFMAN, A. NAGEL, P. GREIL and G. PETZOW, *ibid*. **72** (1989) 765.
19. M. E. BRITTO, Y. BANDO, M. MITOMO and S. SAITO, *J. Mater. Sci*. **29** (1994) 250.
20. Y. MURAKAMI (ed.), "Stress Intensity Factors Handbook," Vol. 1 (Pergamon Press, UK, Oxford, 1987) p. 9.
21. J. R. DRYDEN, D. KUCEROVSHY, D. S. WILKINSON and D. F. WATT, *Acta Metall*. **37** (1989) 2007.
22. M. M. CHADWICK, D. S. WILKINSON and J. R. DRYDEN, *J. Amer. Ceram. Soc*. **75** (1992) 2327.
23. R. RAJ and C. K. CHYUNG, *Acta Metall*. **29** (1981) 159.
24. S. M. WIEDERHORN, B. J. HOCKEY, R. F. KRAUSE, JR. and K. JAKUS, *J. Mater. Sci*. **21** (1986) 810.
25. M. K. FERBER, M. G. JENKINS, T. A. NOLAN and R. L. YECKLEY, *J. Amer. Ceram. Soc*. **77** (1994) 657.
26. F. C. MONKMAN and N. J. GRANT, *Proc. Amer. Soc. Test. Mater*. **56** (1956) 593.
27. F. R. LARSON and J. MILLER, *Trans. ASME* **74** (1952) 765.
28. M. MASUDA, T. MAKINO, Y. NAKASUJI and M. MATSUI, in "Fracture Mechanics of Ceramics," edited by R. C. Bradt et al., Vol. 9 (Plenum Publ. Corp., New York, 1992) p. 481.
29. S. M. WIEDERHORN, J. D. FRENCH and W. E. LUECKE, in "Ceramic Materials and Components for Engines," edited by D. S. Yan, X. R. Fu and S. X. Shi (World Scientific, Singapore, 1994) p. 145.

Received 23 December 1997
and accepted 11 November 1998